A novel role for the C-terminal domain of the influenza A virus host shutoff endoribonuclease PA-X in mediating rapid turnover of the PA-X protein

Rachel Emily Levene[a,b], Shailab D. Shrestha[a,b], Marta Maria Gaglia[a,b #]

[a]Graduate Program in Molecular Microbiology, Tufts University Graduate School of Biomedical Sciences, Boston, MA, USA

[b]Department of Molecular Biology and Microbiology, Tufts University School of Medicine, Boston, MA, USA

[#]Send correspondence to:

Marta Maria Gaglia (marta.gaglia@tufts.edu)

Key Words: influenza A virus, PA-X, host shutoff, protein turnover

Running Title: The influenza A virus RNase PA-X is unstable

Abstract Word Count: 190

Main Text Word Count: 4,963

ABSTRACT:

The influenza A endoribonuclease PA-X regulates virulence and transmission of the virus by reducing host gene expression and thus regulating immune responses to influenza A virus. Despite this key function in viral biology, the levels of PA-X protein remain markedly low during infection, and previous results suggest that these low levels are not solely the result of regulation of the level of translation and RNA stability. How PA-X is regulated post-translationally remains unknown. We now report that the PA-X protein is rapidly turned over. This instability is conserved across multiple viral strains, although the half-life of PA-X from different strains varies, ranging from 30 minutes to a few hours. Moreover, sequences in the variable PA-X C-terminal domain regulate PA-X half-life. Interestingly, we find that the PA-X from the 2009 pandemic H1N1 strain has a longer half-life compared to the other variants we tested. This PA-X isoform has been reported to have a higher host shutoff activity, suggesting a role for protein turnover in regulating PA-X activity. Collectively, this study reveals a novel regulatory mechanism of PA-X protein levels that may impact host shutoff activity during influenza A virus infection.

33 **IMPORTANCE**

34 The PA-X protein from influenza A virus reduces host immune responses to infection through
35 suppressing host gene expression, including genes encoding the antiviral response. Thus, it plays
36 a central role in influenza A virus biology. Despite its key function, PA-X was only discovered
37 in 2012 and much remains to be learned including how PA-X activity is regulated to promote
38 optimal levels of viral infection. In this study we reveal that PA-X protein levels are very low
39 because of rapid turnover. We show that instability is a conserved property among PA-X variants
40 from different strains of influenza A virus, but that the half-lives of PA-X variants differ.
41 Moreover, the longer half-life of PA-X from the 2009 pandemic H1N1 strain correlates with its
42 reported higher activity. Therefore, PA-X stability may be a way to regulate its activity and may
43 contribute to the differential virulence of influenza A virus strains.

44 **INTRODUCTION:**

45 Viruses employ multiple strategies to block host antiviral defenses. In many viruses, this
46 inhibition is partly achieved through a blockade of host gene expression, a process termed "host
47 shutoff". One of the ways influenza A virus induces host shutoff is through the activity of a viral
48 endoribonuclease (RNase), PA-X (1–3). The RNase activity of PA-X results in global changes in
49 the cellular transcriptome (3, 4), while viral mRNAs and genomic RNAs escape PA-X
50 degradation (5). Influenza A viruses engineered to lack PA-X trigger a more potent innate
51 immune and inflammatory response in mice, chickens, and pigs, presumably because of
52 decreased host shutoff (1, 6–10). These results indicate that PA-X controls immune responses *in*
53 *vivo.* More recently, a role for PA-X in transmission has also been established (11, 12). Despite
54 its clear *in vivo* role, much remains to be determined about PA-X biology during infection. PA-X
55 was discovered in 2012 and studies to date have primarily focused on dissecting its mechanism
56 of action, including how subsets of RNAs, including viral RNAs, escape PA-X degradation.
57 Whether and how PA-X activity itself is regulated has not been explored in detail. One study
58 found that co-translational N-terminal acetylation is required for PA-X host shutoff activity (13),
59 but whether there are other co- and post-translational regulatory mechanisms remains unknown.
60 Interestingly, prolonged PA-X expression may be cytotoxic, as shown in yeast by Oishi *et al.*
61 (13, 14). While this is not surprising given its widespread downregulation of RNAs, this
62 observation underscores the idea that PA-X activity may need to be regulated during infection to
63 prevent premature death of the infected cells.

64

65 One way to regulate or limit PA-X activity could be to keep pools of active PA-X protein low in
66 the infected cell. Indeed, PA-X protein levels are remarkably low during infection. Metabolic

67 labeling of nascent proteins in influenza A virus infected cells showed that the levels of PA-X
68 are barely above the limit of detection and lower than other influenza proteins, including the
69 well-known host shutoff factor NS1 (1). These low levels are in part due to how PA-X is
70 produced. PA-X production requires a programmed +1 ribosomal frameshift during translation of
71 segment 3, which encodes the polymerase acidic (PA) subunit of the viral RNA dependent RNA
72 polymerase (RdRp) (1, 15). Only a small percentage of translational runs result in frameshifting
73 and produce PA-X, which has the same N-terminal RNase domain as PA (PA-X amino acids (aa)
74 1-191) and a unique C-terminal domain known as the "X-ORF" (PA-X aa 192-232 or 192-252
75 depending on the strain) (1). Of note, despite this non-canonical production mechanism, PA-X is
76 present in all influenza A virus isolates (16) demonstrating its importance in influenza A virus
77 biology. However, the mechanism of PA-X production does not entirely explain the low levels of
78 PA-X. Indeed, PA-X levels are also low or undetectable when PA-X is expressed ectopically
79 from a construct in which a single nucleotide has been deleted to mimic the frameshift and all
80 translational runs produce PA-X (17). The low levels are also not because PA-X degrades and
81 limits the levels of its own mRNA, as mutating the PA-X catalytic residues D108 or K134 in this
82 ectopic expression system does not increase PA-X levels dramatically (3, 17). This suggests that
83 PA-X levels may be regulated at the level of protein stability.
84
85 Regulation of stability is a well-established post-translational mechanism of protein regulation.
86 For example, Kosik *et. al* established a role for protein turnover in the regulation of the
87 immunomodulatory activity of PB1-F2, another influenza A virus virulence factor (18). PB1-F2
88 inhibits induction of the antiviral cytokine interferon beta (IFN-β) and increases the activity of
89 the viral RdRp (19–21). Mutating the residues required for PB1-F2 ubiquitination and rapid

90 turnover increases PB1-F2 protein levels, which results in a stronger inhibition of IFN-β
91 induction (18). Similarly, regulation of PA-X at the level of protein stability could modulate the
92 host shutoff activity of influenza A virus.
93
94 Previous observations suggest that the X-ORF may regulate the levels of the PA-X protein, as
95 ectopic expression of the N-terminal domain of PA-X results in much higher protein levels than
96 ectopic expression of either wild type (wt) or catalytically inactive PA-X (17). This is not due to
97 changes in frameshifting, as this ectopic expression construct has a nucleotide deletion to mimic
98 the frameshift and only encodes PA-X. A role for the X-ORF in post-translational control of PA-
99 X levels and activity would explain why almost all influenza A strains encode a PA-X protein
100 that has a 61 or 41-aa X-ORF (16) even though only the first 15 aa of the X-ORF are required for
101 PA-X shutoff activity in cells (3, 17, 22). Moreover, most of the sequence variation among PA-X
102 from different strains occurs after the 15th amino acid of the X-ORF, and the strength of PA-X
103 activity has been reported to vary among strains (17, 23, 24). Therefore, we hypothesized that the
104 later portion of the X-ORF and the sequence variation in this region have a regulatory effect on
105 PA-X levels and host shutoff activity.
106
107 Here we report the first investigation of post-translational regulation of PA-X protein levels. We
108 find that PA-X is markedly unstable and identify a region of the X-ORF that regulates PA-X
109 turnover. Additionally, as the X-ORF sequences vary among influenza A virus strains, we find
110 that the half-life of PA-X differs among strains, even though all the PA-X variants tested have
111 generally short half-lives. Interestingly, of the variants we tested, PA-X from the 2009 pandemic
112 H1N1 strain had the longest half-life, which may explain its reported higher host shutoff activity

113 (17, 23, 24). Thus, modulation of PA-X stability may be a mechanism used to regulate PA-X
114 host shutoff activity in different strains and may contribute to influenza A pathogenesis.
115
116 **RESULTS**
117 **PA-X is unstable**
118 Several observations suggested to us that PA-X may be unstable. PA-X is expressed at low levels
119 not only during infection (1), but also during ectopic overexpression from a high expression
120 CMV promoter [(17), our unpublished observations]. Furthermore, ectopic overexpression of the
121 N-terminal RNase domain from the same high expression CMV promoter results in much higher
122 protein levels (17). While the RNase domain in isolation is inactive in cells (3, 5, 17, 22), the
123 differences in protein levels are not due to the loss of activity, because expressing a catalytically
124 inactive version of PA-X still results in markedly low PA-X expression levels (3, 17). Thus, we
125 sought to directly test if PA-X is rapidly turned over. To determine the half-life of the PA-X
126 protein, we performed a cycloheximide chase in human embryonic kidney (HEK) 293T cells
127 transfected with a C-terminally myc tagged PA-X from the influenza A virus strain A/Puerto
128 Rico/8/1934 H1N1 (PR8) containing the D108A mutation in the RNase active site. This mutation
129 abolishes PA-X catalytic activity and host shutoff function (3, 5). We chose to use catalytically
130 inactive PA-X for this experiment and throughout this study to eliminate any confound from
131 changes in host gene expression or PA-X mRNA levels as a result of PA-X activity.
132 Additionally, to make sure any differences in PA-X protein levels are due to changes in turnover
133 and not frameshifting, in this experiment and throughout this study we used PA-X expression
134 constructs where all translational runs produce PA-X, as a single nucleotide was deleted to
135 mimic the frameshift. After treating PA-X-expressing cells with cycloheximide to inhibit

136 translation, we analyzed PA-X protein levels at 0, 15, 30, 60, and 120 minutes after
137 cycloheximide addition by western blotting. Strikingly, PA-X was almost completely gone one
138 hour after the addition of cycloheximide (Fig 1A and 1B), suggesting that PA-X is markedly
139 unstable. By contrast, levels of PA-X mRNA did not decrease throughout the cycloheximide
140 time course (Fig 1C), confirming that the decrease in PA-X protein levels is not due to changes
141 in transcript levels. Based on regression analysis, we calculated a half-life of 86 minutes for PR8
142 PA-X (Fig 1B, Table 1). This is low compared to the half-life of other influenza proteins. For
143 example, the host shutoff factor NS1 from PR8 has a half-life of over 24 hours (25) and PR8
144 PB1-F2 has a half-life of 6.5 hours (26). In addition, human proteins have a median half-life of
145 8.7 hours (27). Together, these data show that PA-X is rapidly turned over compared to other
146 viral and host proteins.
147
148 **The X-ORF mediates PA-X instability**
149 Because ectopic overexpression of the N-terminal domain of PA-X results in higher protein
150 levels than overexpression of full length PA-X (17), we decided to test whether the X-ORF
151 controls PA-X stability. We thus measured the half-life of a truncated version of the catalytically
152 inactive PR8 PA-X that ended after aa 16 of the X-ORF ("PA-X16", Fig 2A). We chose to test
153 PA-X16 instead of the RNase domain alone because truncation of the whole X-ORF results in
154 loss of nuclear localization of PA-X (5, 17). In contrast, PA-X mutants retaining at least 15 aa of
155 the X-ORF are primarily localized to the nucleus, like full-length PA-X (17). Additionally, we
156 and others have previously shown that the first 15 residues of the X-ORF are necessary and
157 sufficient for host shutoff activity (3, 17, 22). Thus, using the PA-X16 truncation should exclude
158 potential confounding factors, such as changes in subcellular localization or in protein-protein

159 interactions needed for activity. In contrast to the rapid decrease in the levels of full-length PA-X
160 (PA-X61) after cycloheximide addition, the protein levels of PA-X16 remained constant
161 throughout the two-hour time course (Fig 2B and 2C). This result shows that PA-X16 is more
162 stable than the full-length protein. There were also no significant changes in the mRNA levels of
163 PA-X16 throughout the time course (Fig 2D). Together, these results indicate that sequences in
164 the X-ORF after the 16th residue are responsible for the instability of PA-X. Since the first 15
165 amino acids of the X-ORF are necessary and sufficient for host shutoff activity (3, 5, 17, 22),
166 these data also suggest that the portions of the X-ORF involved in mediating host shutoff activity
167 and stability are different.
168
169 **The half-life of PA-X varies among strains**
170 Although all influenza A virus strains are predicted to encode PA-X, the sequence of PA-X
171 varies across strains, particularly in the unique C-terminal X-ORF (16). To make sure that the
172 instability we observed is not specific to the X-ORF sequence of PR8 PA-X, we sought to
173 determine if this phenotype was conserved among PA-X from other strains of influenza A virus.
174 We created catalytically inactive D108A mutants in the PA-X from a 2009 pandemic H1N1
175 strain, A/California/7/2009pdm (pH1N1), a lab-adapted H3N2 strain, A/Udorn/307/1972
176 (Udorn), a seasonal H3N2 strain, A/Perth/16/2009 (Perth), and a pre-pandemic seasonal H1N1
177 strain, A/Hong Kong/218847/2006 (HK06), all with a C-terminal myc tag. Tagging all variants
178 with the same tag allows us to compare among strains since many antibodies against influenza
179 proteins only recognize a particular strain or serotype. PA-X from Udorn and HK06 were as or
180 more unstable than PR8 PA-X, with half-lives of 34 and 83 minutes, respectively (Fig 3A, 3B,
181 3D, 3E, Table 1). In contrast, PA-X from Perth was slightly more stable, with a calculated half-

182 life of 250 minutes (4.2 hrs, Fig 3G, 3H, Table 1). PA-X from pH1N1 was significantly more
183 stable, as its levels remained constant throughout the cycloheximide time course (Fig 3J, 3K,
184 Table 2). That said, after four hours of cycloheximide treatment, pH1N1 PA-X protein levels
185 decreased by half (Fig 3M and 3N), suggesting it may also have a shorter half-life than the
186 average human protein (~9 hrs) (27). In all cases, there were no significant decreases in mRNA
187 levels of PA-X from any of the strains (Fig 3C, 3F, 3I, 3L, 3O), again confirming that the
188 decrease in PA-X protein levels are not due to changes in transcript levels. Together, these data
189 show that instability is a conserved property among PA-X variants, but that there are differences
190 in PA-X half-life among strains. Moreover, the pH1N1 PA-X is substantially longer lived than
191 other variants.
192
193 **The length difference between the two major variants of the PA-X X-ORF does not account**
194 **for differences in PA-X instability**
195 There are two main variants of PA-X in influenza A strains distinguishable by their protein
196 lengths: one is 252-aa long, with an X-ORF of 61 aa, and the other is 232-aa long, with an X-
197 ORF of 41 aa (16). The PA-X variants in PR8, Perth, Udorn and HK06 all have a 61-aa X-ORF,
198 like most human strains, while the pH1N1 PA-X has a 41-aa X-ORF, which is otherwise found
199 in a subset of swine and canine strains (16). Although some studies have suggested that the
200 length of the X-ORF may regulate activity (12, 28, 29), it is still unclear exactly what the
201 function of the additional 20 aa is. Since pH1N1 PA-X has a much longer half-life than most of
202 the other PA-X isoforms we tested (Fig 3K, Table 1), we wondered if the shorter X-ORF
203 accounted for the difference in stability. We thus tested the half-life of a truncated version of
204 catalytically inactive PR8 PA-X that ended after the 41st amino acid (Fig 4A), which we termed

205 “PA-X41”. Despite the truncation, PR8 PA-X41 protein levels rapidly decreased after translation
206 inhibition (Fig 4B and 4C), with a half-life of 99 minutes. This is not significantly different from
207 that of full length PR8 PA-X (PA-X61) (p = 0.8118) (Fig 4C). We note that we consistently
208 detected a double band in cells expressing PR8 PA-X41. While the reason for this doublet is
209 currently unknown, we note that a similar doublet was also apparent in the staining for pH1N1
210 PA-X in Hayashi *et al.* (17). There were no significant decreases in the mRNA levels of PR8
211 PA-X41 (Fig 4D), confirming that the decrease in PR8 PA-X41 protein levels is not due to
212 changes in transcript levels. Thus, the distal 20 residues likely do not play a role in protein
213 stability, and other sequence differences between PR8 and pH1N1 PA-X control their turnover
214 rates.
215
216 **PA-X host shutoff activity in infected cells is reduced upon translational inhibition**
217 To confirm that PA-X is unstable in the context of influenza A virus infection we first attempted
218 to measure its half-life in PR8-infected cells using an antibody against PA that has been
219 previously used to detect PR8 PA-X (30). However, like Rigby *et al.* (30), we observed a large
220 number of bands in the section of the blot corresponding to the predicted molecular weight of
221 PA-X, and were unable to reliably and reproducibly identify the band corresponding to PA-X.
222 Unfortunately, we cannot tag PA-X in the context of the virus. The C-terminus cannot be tagged
223 because it overlaps with the coding sequence for the C-terminus of PA (1, 15). N-terminal tags
224 reduce PA activity and viral replication (31, 32), and are also expected to reduce the activity of
225 PA-X because of the importance of its N-terminal acetylation (13). Therefore, we sought another
226 way to look for evidence of PA-X instability during infection and used PA-X activity in the
227 presence of cycloheximide as a proxy for rapid changes in PA-X protein levels. We reasoned that

228 if levels of PA-X are quickly depleted after halting translation with cycloheximide, there will be
229 less PA-X host shutoff activity in cells. To confirm this, we first tested PA-X host shutoff
230 activity in the presence of cycloheximide in A549 cells that inducibly overexpress either wt PR8
231 PA-X or the catalytically inactive PR8 PA-X D108A mutant. These cells allow us to measure
232 changes in the RNA levels of endogenous genes (3, 5). Following overnight induction of PA-X
233 expression and a 2-hour cycloheximide treatment, we analyzed levels of G6PD and TAF7 RNA,
234 representative PA-X targeted and resistant RNAs, respectively (3). Levels of G6PD significantly
235 decreased upon PA-X expression, but this decrease was not observed in PA-X-expressing cells
236 treated with cycloheximide (Fig 5A). In contrast, cycloheximide had no effect on the levels of
237 G6PD in cells expressing catalytically inactive PA-X or levels of the PA-X resistant RNA TAF7
238 (Fig 5A), confirming that the effect of cycloheximide on RNA levels was linked to PA-X
239 activity. Furthermore, PA-X mRNA levels did not decrease with cycloheximide, confirming that
240 any changes in PA-X host shutoff activity are not the result of changes in PA-X transcript levels
241 (Fig 5A).
242
243 We then performed the same experiment in A549 cells infected with either wt PR8 or PA-X-
244 deficient PR8 virus (ΔX). PR8 ΔX carries mutations in the frameshifting site in segment 3 that
245 reduce PA-X production, as well as a nonsense mutation at PA-X aa 201, which abolishes
246 activity of any residual PA-X (3). At 24 hours post-infection, we analyzed levels of G6PD and
247 TAF7 mRNA after a 2-hour cycloheximide treatment. As expected, G6PD levels were
248 significantly lower in wt PR8-infected cells compared to PR8 ΔX-infected cells due to PA-X
249 mediated host shutoff (Fig 5B), while the levels of the PA-X-resistant RNA TAF7 were similar.
250 However, the difference in G6PD levels was not detected in infected cells treated with

251 cycloheximide, suggesting that cycloheximide treatment prevents PA-X-mediated host shutoff,
252 presumably due to rapid loss of PA-X expression (Fig 5B). Conversely, PA-X had no effect on
253 TAF7 levels. There were no significant changes in the RNA levels of the viral gene HA during
254 cycloheximide treatment, confirming that the decrease in PA-X activity is not the result of
255 changes in viral replication (Fig 5B). Thus, while we cannot confirm that PA-X protein levels
256 significantly decrease in infected cells after a translational block, we do observe markedly
257 reduced PA-X activity. Taken together with the decrease in both PA-X protein levels (Fig 1) and
258 PA-X activity (Fig 5A) during ectopic overexpression, our results indicate that the reduction in
259 PA-X activity during infection is likely the result of decreased PA-X protein levels. Therefore, it
260 is likely that PA-X is rapidly turned over during infection.
261

262 **DISCUSSION**

263 The PA-X protein is present at low levels in influenza A virus-infected cells, which has been
264 generally assumed to be due to its production mechanism based on ribosomal frameshifting.
265 However, we have found that PA-X protein levels are also regulated at the post-translational
266 level, and that PA-X is rapidly turned over (Fig 1, 3, 5). We show that PA-X aa 208-232 (aa 17-
267 41 of the X-ORF) contain a stability-regulating sequence, as truncating PA-X at aa 232 does not
268 change its half-life (Fig 4), while truncating it at aa 207 significantly increases it (Fig 2). Our
269 results also indicate that instability is a conserved property of PA-X protein, but that differences
270 in PA-X sequence among the strains lead to different half-lives (Fig 3). We propose that this
271 post-translational regulation results in low steady-state levels of PA-X protein in infected cells,
272 which in turn may limit the active pool of PA-X. Given that PA-X is already made at low levels

273 during infection, the instability of this protein suggests that limiting PA-X activity is of
274 paramount importance for viral replication.
275
276 It is still unknown how PA-X is degraded by the cell. We previously identified interactions
277 between the X-ORF of both PR8 and pH1N1 PA-X and host proteins involved in protein
278 turnover, including three components of the proteasome, PSME3, PSMD3, and PSMC5, and a
279 ubiquitin E3 ligase, HUWE1 (3). While components of the proteasome are often found as
280 contaminants in proteomics studies, the identification of an E3 ligase as an interactor increases
281 confidence in the identification of the proteasome and suggests a role for proteasomal
282 degradation. Understanding the role of HUWE1 and the ubiquitin-proteasome system in
283 regulation of PA-X protein levels is a current avenue of investigation.
284
285 It is attractive to think that by rapidly turning over the pool of active PA-X in the cell, instability
286 could serve as a mechanism to control PA-X host shutoff activity. Prolonged PA-X activity
287 could in theory have catastrophic consequences not only for the cell but also for successful viral
288 infection. We have observed that prolonged, high level PA-X expression kills human cells (data
289 not shown), as reported by Oishi *et al.* in yeast (13, 14). This cytopathic effect could be due to
290 the activation of cellular stress response pathways as a response to prolonged widespread RNA
291 degradation, or to a direct effect of the RNA degradation on the levels of unstable proteins that
292 keep the cell alive, like the Bcl-2 family member MCL-1 (33). During infection, this toxicity
293 could prematurely kill the infected cell before progeny virions are made, which would curtail
294 viral replication. In support of this, our group previously found that the X-ORF from PR8 PA-X
295 truncated to 16 amino acids may have stronger activity on a co-transfected reporter compared to

296 full length PR8 PA-X, although the difference was not statistically significant (3). Additionally,
297 the Takimoto lab showed that truncation of the pH1N1 PA-X X-ORF to 15 residues in the virus
298 (through a premature stop codon) increased host shutoff during infection (17). Thus, the X-ORF
299 may curtail PA-X activity by reducing its protein levels, although the link between PA-X
300 stability, host shutoff activity and virulence remains to be rigorously tested during infection.
301
302 Our study implicates the middle portion of the X-ORF in the regulation of PA-X stability. With
303 the exception of a few equine H7N7 and bat influenza strains, all influenza A strains have PA-X
304 with X-ORFs of 41 or 61 amino acids (16). However, there are other locations where a stop
305 codon could have evolved without changes to the PA reading frame (16), and only the first 15
306 amino acids of the X-ORF are required for host shutoff activity (3, 17, 22). Therefore, the fact
307 that sequences beyond aa 15 are nonetheless retained through evolution suggests that these
308 additional sequences have a necessary function despite being dispensable for activity. Our study
309 implies that the rest of the X-ORF may be needed to regulate PA-X, and in particular to ensure
310 that PA-X is rapidly turned over (Fig 2). A post-translational mechanism to control PA-X protein
311 levels may be important to limit activity, because in the context of infection PA-X does not
312 cleave its own transcript and thus does not autoregulate its expression (5). This is in contrast to
313 other viral host shutoff RNases like the alphaherpesvirus protein vhs, which is thought to be able
314 to target its own transcript (34). If hyperactive PA-X is detrimental to viral fitness, there may be
315 selective pressure to maintain the instability of PA-X, and thus retain the later portion of the X-
316 ORF even though it is not required for host shutoff activity.
317
318 It was surprising that the protein decay rate of pH1N1 PA-X was dramatically different from that

319 of most other strains (Fig 3). This is particularly striking given that the biggest difference
320 between pH1N1 and the other tested strains is the absence of the 20 distal amino acids, but we
321 find that this is not responsible for the reduced degradation (Fig 4). PA-X from strains with avian
322 origin PA segments, like that of pH1N1 (35), has been reported to have higher host shutoff
323 activity compared to PA-X from strains with human-adapted PA segments (23). This has raised
324 the possibility that PA-X host shutoff activity is linked to virulence and pathogenicity (36).
325 Given that pH1N1 PA-X accumulates to higher levels in the cell when compared to its
326 counterparts from PR8, Udorn, and HK06 (Fig 1 and 3), which are human-adapted, it is possible
327 that strain-specific differences in PA-X activity may be the result of strain-specific differences in
328 stability. This is an interesting relationship, especially given the higher virulence of a mouse
329 adapted pH1N1 strain when compared to PR8 (37). It will be important to assess the functional
330 consequences of PA-X stability and what it means for PA-X host shutoff activity and viral
331 pathogenesis.
332
333 Collectively our results reveal for the first time that PA-X is markedly unstable. The stability of
334 different PA-X variants may control host shutoff activity, which could have consequences for
335 virulence and pathogenesis. Since the region of PA-X regulating stability is maintained despite
336 not being required for host shutoff, having an unstable PA-X may be advantageous for the virus
337 and be selected for during evolution. Further elucidation of the mechanism of PA-X turnover in
338 the infected cell and its functional consequences will uncover important aspects of PA-X biology
339 and regulation of host shutoff, allowing us to further link PA-X activity with influenza A virus
340 virulence and pathogenesis.

341 **ACKNOWLEDGEMENTS**

342 We thank Dr. Seema Lakdawala, Dr. Jesse Bloom and Dr. Richard Webby for constructs, and
343 members of the Moore and Bohm lab and Malavika Raman for suggestions and feedback. We
344 also thank Dr. Denys Khaperskyy, Dr. Craig McCormick and members of the Gaglia lab for
345 suggestions, feedback, and critical reading of the manuscript. This work was supported by NIH
346 grant R01 AI137358 to M.M.G. R.E.L. was supported by NIH training grant T32 AI007422.
347 S.D.S. is a David J. Cosman, Ph.D. fellow in the Tufts Molecular Microbiology program.

348 **MATERIALS AND METHODS**

349 **Plasmids**

350 pCR3.1-PR8-PA-X-D108A-myc was previously described (5, 38). pCR3.1-PA-X D108A-myc
351 constructs for A/California/7/2009pdm, A/Udorn/307/1972, and A/Hong Kong/218847/2006
352 were generated from the corresponding previously described wild-type plasmids (3, 5) by site-
353 directed mutagenesis. The indicated PA-X coding regions were PCR-amplified using primers in
354 Table 2 and inserted into the SalI and XhoI sites of a pCR3.1-C-terminal-myc backbone.
355 pCR3.1-PA-X-D108A-myc constructs for A/Perth/16/2009 (Perth) was generated by subcloning
356 the PA-X coding region from the plasmid from segment 3 for this strain (a kind gift from Dr.
357 Seema Lakdawala). The Perth PA-X coding region was PCR-amplified using primers in Table 2
358 to delete a base (which mimics the frameshift) and insert the D108A mutation. It was then
359 inserted into the SalI and MluI sites of a pCR3.1-C-terminal-myc backbone. pCR3.1-PR8-PA-
360 X16-D108A-myc and pCR3.1-PR8-PA-X41-D108A-myc were generated by PCR-amplifying
361 the truncated coding region from pCR3.1-PA-X-PR8-D108A-myc using primers in Table 2. The
362 truncated regions were then inserted into the SalI and MluI sites of a pCR3.1-C-terminal-myc
363 backbone. Gibson cloning using HiFi assembly mix (New England Biolabs) was used to make
364 all constructs.

365

366 **Cell lines, transfections, and drug treatments**

367 Human embryonic kidney (HEK293T) cells (ATCC), Madin-Darby Canine Kidney (MDCK)
368 cells (ATCC), A549 (ATCC) cells and derivatives were cultured in Dulbecco's modified Eagle's
369 medium (DMEM; Life Technologies) supplemented with 10% fetal bovine serum (Hyclone) and
370 maintained at 37°C in 5% CO_2 atmosphere. A549 cell lines expressing PA-X under a

371 doxycycline-inducible promoter (A549-iPA-X_PR8_wt#1 and A549-iPA-X_PR8_D108A#8)
372 were previously described (5). For all 2-hour half-life experiments, HEK293T cells were plated
373 in 10-cm dishes and transfected with 12 µg total DNA (including 6 µg of PA-X construct) using
374 JetPrime (Polyplus transfection). 6 hours post transfection, cells were transferred to 6-well
375 plates, and one well was set up per indicated time point. For the indicated 4-hour cycloheximide
376 experiments, HEK293T cells were plated in 2 6-wells for each indicated strain and transfected
377 with 2 µg of DNA (including 1 µg of PA-X construct) per well using JetPrime (Polyplus
378 transfection). 6 hours post transfection, the 2 wells for each construct were trypsinized, mixed
379 together, and replated into 2 wells. 24 hours post transfection, cells were treated with 200 µg/mL
380 of cycloheximide (Sigma Aldrich) or dH_2O as vehicle control, and collected for RNA and
381 protein isolation at the indicated time points. For experiments using iPA-X cells, cells were
382 treated with 0.5 µg/mL doxycycline (Thermo Fisher) for 14 hours to induce PA-X expression
383 and then 200 µg/mL of cycloheximide (or vehicle control, dH_2O) for 2 hours prior to RNA
384 collection.
385
386 **Viruses and Infections**
387 Wild type influenza A virus A/Puerto Rico/8/1934 H1N1 (PR8) and the mutant PR8 ΔX were
388 generated as previously described in (3) using the 8-plasmid reverse genetic system (39). Viral
389 stocks were produced in MDCK cells and infectious titers were determined by plaque assay in
390 MDCKs using a 1.2% Avicel overlay described in Matrosovich *et al.* (40). A549 monolayers
391 were mock infected or infected with the wild-type or PA-X mutant viruses at a MOI = 5 for 1 hr
392 at 37°C. Monolayers were washed with PBS, and fresh infection media (0.5% Bovine Serum
393 Albumin (BSA; Sigma Aldrich) in DMEM supplemented with 0.5 µg/mL of L-(tosylamido-2-

394 phenyl) ethyl chloromethyl ketone (TPCK)-treated trypsin) (Sigma Aldrich) was added and cells
395 were incubated at 37°C in 5% CO_2 atmosphere for 24 hours prior to cycloheximide treatment.
396
397 **RNA purification, cDNA preparation and RT-qPCR**
398 RNA was extracted from cells and purified using the Quick-RNA Miniprep kit (Zymo Research),
399 following manufacturer's protocol. In all cases, the RNA was treated with Turbo DNase (Life
400 Technologies), then reverse transcribed using iScript supermix (Bio-Rad) per manufacturer's
401 protocol. qPCR was performed using iTaq Universal SYBR Green supermix (Bio-Rad), on the
402 Bio-Rad CFX Connect Real-Time System qPCR and analyzed with Bio-Rad CFX Manager 3.1
403 Program. The primers used are listed in Table 2.
404
405 **Protein extraction, western blotting and antibodies**
406 Total cellular protein was collected in protein lysis buffer (50 mM Tris-HCl pH 7.4, 150 mM
407 NaCl, 2 mM EDTA, 0.5% sodium deoxycholate, 0.5% SDS, 1% NP-40) supplemented with
408 cOmplete EDTA-free protease inhibitor cocktail (Roche) and 1 U/mL benzonase nuclease
409 (Sigma Aldrich). The benzonase is included to degrade DNA and promote release of PA-X from
410 the nucleus. Proteins were separated on 12% SDS-PAGE gels and transferred onto 0.22 μm
411 PVDF membranes (Millipore). Western Blots were performed in PBST with 0.5% milk using
412 antibodies against the Myc tag (1:1000, Cell Signaling Technologies 2276), and human β-tubulin
413 (1:1000, Cell Signaling Technologies 2128). Secondary antibodies conjugated to HRP were
414 purchased from Southern Biotechnologies (rabbit, OB4030-05; mouse, OB1031-05) and used at
415 1:5,000 dilution. Membranes were developed using Pierce ECL Western blotting substrate

416 (Thermo Fisher) and imaged with a Syngene G:Box Chemi XT4 gel doc system. Images were
417 quantified using GeneTools version 4.3.8.0
418
419 **Statistical Analysis**
420 All statistical analysis was performed using GraphPad Prism version 8.0 for Mac OS X,
421 (GraphPad Software, San Diego, CA, USA). For half-lives experiments, statistical significance
422 was determined by performing linear regression and comparing slopes and intercepts. For other
423 experiments, statistical significance was determined by Student's *t*-test, or analysis of variance
424 (ANOVA) followed by a *post-hoc* multiple comparisons test (Sidak's or Tukey's) as indicated. A
425 minimum of three biological replicates were conducted for all experiments.

426 **References**

427 1. Jagger BW, Wise HM, Kash JC, Walters K-A, Wills NM, Xiao Y-L, Dunfee RL,
428 Schwartzman LM, Ozinsky A, Bell GL, Dalton RM, Lo A, Efstathiou S, Atkins JF, Firth
429 AE, Taubenberger JK, Digard P. 2012. An Overlapping Protein-Coding Region in
430 Influenza A Virus Segment 3 Modulates the Host Response. Science 337:199–204.

431 2. Levene RE, Gaglia MM. 2018. Host Shutoff in Influenza A Virus: Many Means to an End.
432 Viruses 10:475.

433 3. Gaucherand L, Porter BK, Levene RE, Price EL, Schmaling SK, Rycroft CH, Kevorkian Y,
434 McCormick C, Khaperskyy DA, Gaglia MM. 2019. The Influenza A Virus
435 Endoribonuclease PA-X Usurps Host mRNA Processing Machinery to Limit Host Gene
436 Expression. Cell Reports 27:776-792.e7.

437 4. Chaimayo C, Dunagan M, Hayashi T, Santoso N, Takimoto T. Specificity and functional
438 interplay between influenza virus PA-X and NS1 shutoff activity 26.

439 5. Khaperskyy DA, Schmaling S, Larkins-Ford J, McCormick C, Gaglia MM. 2016. Selective
440 Degradation of Host RNA Polymerase II Transcripts by Influenza A Virus PA-X Host
441 Shutoff Protein. PLOS Pathogens 12:e1005427.

442 6. Gao H, Sun Y, Hu J, Qi L, Wang J, Xiong X, Wang Y, He Q, Lin Y, Kong W, Seng L-G,
443 Sun H, Pu J, Chang K-C, Liu X, Liu J. 2015. The contribution of PA-X to the virulence of
444 pandemic 2009 H1N1 and highly pathogenic H5N1 avian influenza viruses. Scientific
445 Reports 5:8262.

446 7. Gong X-Q, Sun Y-F, Ruan B-Y, Liu X-M, Wang Q, Yang H-M, Wang S-Y, Zhang P,
447 Wang X-H, Shan T-L, Tong W, Zhou Y-J, Li G-X, Zheng H, Tong G-Z, Yu H. 2017. PA-X
448 protein decreases replication and pathogenicity of swine influenza virus in cultured cells
449 and mouse models. Veterinary Microbiology 205:66–70.

450 8. Hayashi T, MacDonald LA, Takimoto T. 2015. Influenza A Virus Protein PA-X
451 Contributes to Viral Growth and Suppression of the Host Antiviral and Immune Responses.
452 Journal of Virology 89:6442–6452.

453 9. Hu J, Mo Y, Wang X, Gu M, Hu Z, Zhong L, Wu Q, Hao X, Hu S, Liu W, Liu H, Liu X,
454 Liu X. 2015. PA-X Decreases the Pathogenicity of Highly Pathogenic H5N1 Influenza A
455 Virus in Avian Species by Inhibiting Virus Replication and Host Response. Journal of
456 Virology 89:4126–4142.

457 10. Xu G, Zhang X, Liu Q, Bing G, Hu Z, Sun H, Xiong X, Jiang M, He Q, Wang Y, Pu J, Guo
458 X, Yang H, Liu J, Sun Y. 2017. PA-X protein contributes to virulence of triple-reassortant
459 H1N2 influenza virus by suppressing early immune responses in swine. Virology 508:45–
460 53.

461 11. Sun Y, Hu Z, Zhang X, Chen M, Wang Z, Xu G, Bi Y, Tong Q, Wang M, Sun H, Pu J,
462 Iqbal M, Liu J. 2020. R195K mutation in the PA-X protein increases the virulence and
463 transmission of influenza A virus in mammalian hosts. J Virol JVI.01817-19,
464 jvi;JVI.01817-19v1.

465 12. Liu L, Song S, Shen Y, Ma C, Wang T, Tong Q, Sun H, Pu J, Iqbal M, Liu J, Sun Y. 2020.
466 Truncation of PA-X Contributes to Virulence and Transmission of H3N8 and H3N2 Canine
467 Influenza Viruses in Dogs. J Virol 94:e00949-20, /jvi/94/15/JVI.00949-20.atom.

468 13. Oishi K, Yamayoshi S, Kozuka-Hata H, Oyama M, Kawaoka Y. 2018. N-Terminal
469 Acetylation by NatB Is Required for the Shutoff Activity of Influenza A Virus PA-X. Cell
470 Reports 24:851–860.

471 14. Oishi K, Yamayoshi S, Kawaoka Y. 2018. Identification of novel amino acid residues of
472 influenza virus PA-X that are important for PA-X shutoff activity by using yeast. Virology
473 516:71–75.

474 15. Firth AE, Jagger BW, Wise HM, Nelson CC, Parsawar K, Wills NM, Napthine S,
475 Taubenberger JK, Digard P, Atkins JF. 2012. Ribosomal frameshifting used in influenza A
476 virus expression occurs within the sequence UCC_UUU_CGU and is in the +1 direction.
477 Open Biology 2:120109.

478 16. Shi M, Jagger BW, Wise HM, Digard P, Holmes EC, Taubenberger JK. 2012. Evolutionary
479 Conservation of the PA-X Open Reading Frame in Segment 3 of Influenza A Virus. Journal
480 of Virology 86:12411–12413.

481 17. Hayashi T, Chaimayo C, McGuinness J, Takimoto T. 2016. Critical Role of the PA-X C-
482 Terminal Domain of Influenza A Virus in Its Subcellular Localization and Shutoff Activity.
483 J Virol 90:7131–7141.

484 18. Košík I, Práznovská M, Košíková M, Bobišová Z, Hollý J, Varečková E, Kostolanský F,
485 Russ G. 2015. The Ubiquitination of the Influenza A Virus PB1-F2 Protein Is Crucial for
486 Its Biological Function. PLoS ONE 10:e0118477.

487 19. Varga ZT, Palese P. 2011. The influenza A virus protein PB1-F2. Virulence 2:542–546.

488 20. Varga ZT, Ramos I, Hai R, Schmolke M, García-Sastre A, Fernandez-Sesma A, Palese P.
489 2011. The Influenza Virus Protein PB1-F2 Inhibits the Induction of Type I Interferon at the
490 Level of the MAVS Adaptor Protein. PLoS Pathog 7:e1002067.

491 21. Varga ZT, Grant A, Manicassamy B, Palese P. 2012. Influenza Virus Protein PB1-F2
492 Inhibits the Induction of Type I Interferon by Binding to MAVS and Decreasing
493 Mitochondrial Membrane Potential. J Virol 86:8359–8366.

494 22. Oishi K, Yamayoshi S, Kawaoka Y. 2015. Mapping of a Region of the PA-X Protein of
495 Influenza A Virus That Is Important for Its Shutoff Activity. Journal of Virology 89:8661–
496 8665.

497 23. Desmet EA, Bussey KA, Stone R, Takimoto T. 2013. Identification of the N-Terminal
498 Domain of the Influenza Virus PA Responsible for the Suppression of Host Protein
499 Synthesis. Journal of Virology 87:3108–3118.

500 24. Nogales A, Martinez-Sobrido L, Chiem K, Topham DJ, DeDiego ML. 2018. Functional
501 Evolution of the 2009 Pandemic H1N1 Influenza Virus NS1 and PA in Humans. Journal of
502 Virology 92:e01206-18.

503 25. Santos A, Pal S, Chacón J, Meraz K, Gonzalez J, Prieto K, Rosas-Acosta G. 2013.
504 SUMOylation Affects the Interferon Blocking Activity of the Influenza A Nonstructural
505 Protein NS1 without Affecting Its Stability or Cellular Localization. Journal of Virology
506 87:5602–5620.

507 26. Cheng Y-Y, Yang S-R, Wang Y-T, Lin Y-H, Chen C-J. 2017. Amino Acid Residues 68–71
508 Contribute to Influenza A Virus PB1-F2 Protein Stability and Functions. Front Microbiol
509 8:692.

510 27. Chen W, M. Smeekens J, Wu R. 2016. Systematic study of the dynamics and half-lives of
511 newly synthesized proteins in human cells. Chemical Science 7:1393–1400.

512 28. Gao H, Sun H, Hu J, Qi L, Wang J, Xiong X, Wang Y, He Q, Lin Y, Kong W, Seng L-G,
513 Pu J, Chang K-C, Liu X, Liu J, Sun Y. 2015. Twenty amino acids at the C-terminus of PA-
514 X are associated with increased influenza A virus replication and pathogenicity. Journal of
515 General Virology 96:2036–2049.

516 29. Feng KH, Sun M, Iketani S, Holmes EC, Parrish CR. 2016. Comparing the functions of
517 equine and canine influenza H3N8 virus PA-X proteins: Suppression of reporter gene
518 expression and modulation of global host gene expression. Virology 496:138–146.

519 30. Rigby RE, Wise HM, Smith N, Digard P, Rehwinkel J. 2019. PA-X antagonises MAVS-
520 dependent accumulation of early type I interferon messenger RNAs during influenza A
521 virus infection. Sci Rep 9:7216.

522 31. Hara K, Schmidt FI, Crow M, Brownlee GG. 2006. Amino Acid Residues in the N-
523 Terminal Region of the PA Subunit of Influenza A Virus RNA Polymerase Play a Critical

524 Role in Protein Stability, Endonuclease Activity, Cap Binding, and Virion RNA Promoter
525 Binding. Journal of Virology 80:7789–7798.

526 32. Maier HJ, Kashiwagi T, Hara K, Brownlee GG. 2008. Differential role of the influenza A
527 virus polymerase PA subunit for vRNA and cRNA promoter binding. Virology 370:194–
528 204.

529 33. Adams KW, Cooper GM. 2007. Rapid Turnover of Mcl-1 Couples Translation to Cell
530 Survival and Apoptosis. J Biol Chem 282:6192–6200.

531 34. Elgadi MM, Hayes CE, Smiley JR. 1999. The Herpes Simplex Virus vhs Protein Induces
532 Endoribonucleolytic Cleavage of Target RNAs in Cell Extracts. J Virol 73:7153–7164.

533 35. Garten RJ, Davis CT, Russell CA, Shu B, Lindstrom S, Balish A, Sessions WM, Xu X,
534 Skepner E, Deyde V, Okomo-Adhiambo M, Gubareva L, Barnes J, Smith CB, Emery SL,
535 Hillman MJ, Rivailler P, Smagala J, Graaf M de, Burke DF, Fouchier RAM, Pappas C,
536 Alpuche-Aranda CM, López-Gatell H, Olivera H, López I, Myers CA, Faix D, Blair PJ, Yu
537 C, Keene KM, Dotson PD, Boxrud D, Sambol AR, Abid SH, George KS, Bannerman T,
538 Moore AL, Stringer DJ, Blevins P, Demmler-Harrison GJ, Ginsberg M, Kriner P,
539 Waterman S, Smole S, Guevara HF, Belongia EA, Clark PA, Beatrice ST, Donis R, Katz J,
540 Finelli L, Bridges CB, Shaw M, Jernigan DB, Uyeki TM, Smith DJ, Klimov AI, Cox NJ.
541 2009. Antigenic and Genetic Characteristics of Swine-Origin 2009 A(H1N1) Influenza
542 Viruses Circulating in Humans. Science 325:197–201.

543 36. Lutz MM, Dunagan MM, Kurebayashi Y, Takimoto T. 2020. Key Role of the Influenza A
544 Virus PA Gene Segment in the Emergence of Pandemic Viruses. 4. Viruses 12:365.

545 37. Meunier I, Morisseau O, Garneau É, Marois I, Cloutier A, Richter MV. 2015. Infection
546 with a Mouse-Adapted Strain of the 2009 Pandemic Virus Causes a Highly Severe Disease
547 Associated with an Impaired T Cell Response. PLoS One 10.

548 38. Khaperskyy DA, Emara MM, Johnston BP, Anderson P, Hatchette TF, McCormick C.
549 2014. Influenza A Virus Host Shutoff Disables Antiviral Stress-Induced Translation Arrest.
550 PLOS Pathogens 10:e1004217.

551 39. Hoffmann E, Neumann G, Kawaoka Y, Hobom G, Webster RG. 2000. A DNA transfection
552 system for generation of influenza A virus from eight plasmids. Proceedings of the National
553 Academy of Sciences 97:6108–6113.

554 40. Matrosovich M, Matrosovich T, Garten W, Klenk H-D. 2006. New low-viscosity overlay
555 medium for viral plaque assays. Virol J 3:63.

556

557

558 **FIGURE AND TABLE LEGENDS**

559 **TABLE 1: HALF-LIVES OF PA-X FROM PR8, pH1N1, UDORN, HK06, AND PERTH.** A
560 linear regression was carried out on the quantification plots in Figure 3. The slope of the linear
561 regression line and the calculated half-life are reported. The half-life was calculated as the
562 negative of the inverse of the slope in minutes. Where the 1/slope value yielded a half-life over 2
563 hours, the calculated values are expected to be less accurate. The slope and half-life for PR8 PA-
564 X was calculated based on regression analysis from Figure 1B.

565

566 **TABLE 2: PRIMERS USED IN THIS STUDY.** Primers used in this study for qPCR and
567 cloning.

568

569 **FIGURE 1: PA-X is unstable**.
570 (A-C) Protein and RNA samples were collected from HEK293T cells expressing the catalytically
571 inactive PR8 PA-X at the indicated time points after treatment with 200 μg/mL of cycloheximide
572 (CHX) to inhibit translation. (-) indicates vehicle-treated cells collected at 120 minutes. (A)
573 Representative western blot using anti-myc antibodies to detect myc-tagged PA-X and tubulin as
574 a loading control. (B) Plot of the relative levels of PA-X after cycloheximide treatment. For each
575 replicate, PA-X protein levels were normalized to tubulin protein levels and reported as the $\log_2$
576 transformed ratio relative to time 0. The line represents the linear regression and the shaded
577 region its 95% confidence interval. n = 7 (C) Levels of PA-X mRNA were measured by RT-
578 qPCR. After normalization to 18S rRNA, levels were plotted as amounts relative to time 0. n = 3.

579

580

581 **FIGURE 2: The X-ORF mediates PA-X instability**

582 (A) Schematic diagram of PA-X domains and PR8 PA-X16 truncation used. (B-D) Protein and
583 RNA samples were collected from HEK293T cells expressing the catalytically inactive full-
584 length or truncated C-terminally myc-tagged PA-X at the indicated time points after treatment
585 with 200 μg/mL of cycloheximide (CHX) to inhibit translation. (-) indicates vehicle-treated cells
586 collected at 120 minutes. (B) Representative western blot using anti-myc antibodies to detect
587 myc-tagged PA-X and tubulin as a loading control. (C) Plot of the relative levels of PA-X after
588 cycloheximide treatment. For each replicate, PA-X protein levels were normalized to tubulin
589 protein levels and reported as the $\log_2$ transformed ratio from time 0. A linear regression was
590 performed for each dataset and the *p* value calculated relative to PR8 PA-X61 (full length PA-
591 X). The lines represent the linear regression and the shaded regions indicate the 95% confidence
592 interval (PA-X61: slope = -0.72, confidence interval = -1.04 – -0.39; PA-X16: slope = 0.34,
593 confidence interval = 0.04 – 0.64). The half-life ($t_{1/2}$) for PA-X61 was calculated as the negative
594 inverse of the slope and is reported in minutes. As the slope for PA-X16 is positive, the half-life
595 of this protein cannot be calculated and is therefore reported simply as longer than the time
596 course of the experiment. $n \geq 3$ (D) Levels of PA-X16 mRNA were measured by RT-qPCR.
597 After normalization to 18S rRNA, levels are plotted as amounts relative to time 0. $n > 3$.

598

599 **FIGURE 3: The stability of PA-X varies among influenza A virus strains.**

600 Protein and RNA samples were collected from HEK293T cells expressing the catalytically
601 inactive C-terminally myc tagged PA-X from indicated strain at the indicated time points (A-L)
602 or 4 hours (M-O) after treatment with 200 μg/mL of cycloheximide (CHX) to inhibit translation.
603 (-) indicates vehicle-treated cells collected at 120 minutes (A-L) or 4 hours (M-O). (A, D, G, J,

604 M) Representative western blots using anti-myc antibodies to detect myc-tagged PA-X and
605 tubulin as a loading control. (B, E, H, K) Plot of the relative levels of PA-X after cycloheximide
606 treatment. For each replicate, PA-X protein levels were normalized to tubulin protein levels and
607 reported as the $\log_2$ transformed ratio from time zero. The line represents the linear regression
608 and the shaded region its 95% confidence interval. n = 3 for each variant. In K, the PR8 PA-X
609 dataset from Figure 1 is included for comparison and the *p* value relative to PR8 PA-X is
610 reported. Two of the three pH1N1 PA-X replicates were performed in parallel with PR8 PA-X.
611 (N) Plot of average change in PA-X levels after 4-hour cycloheximide treatment. For each
612 replicate, protein levels of PA-X were normalized to tubulin protein levels and reported as the
613 fold change vs. vehicle-treated PA-X expressing cells. * = $p < 0.05$, Student's *t*-test. n = 3 . (C, F,
614 I, L, O) Levels of PA-X mRNA were measured by RT-qPCR. After normalization to 18S rRNA,
615 levels are plotted as amounts relative to time 0 (C, F, I, L) or as arbitrary units (O). n = 3.
616
617 **FIGURE 4: The length difference between the two major variants of the PA-X X-ORF does**
618 **not account for differences in PA-X instability.**
619 (A) Schematic diagram of PA-X domains and PR8 PA-X41 truncation used. (B-D) Protein and
620 RNA samples were collected from HEK293T cells expressing the catalytically inactive truncated
621 or full-length C-terminally myc-tagged PA-X at the indicated time points after treatment with
622 200 μg/mL of cycloheximide (CHX) to inhibit translation. (-) indicates vehicle-treated cells
623 collected at 120 minutes. (B) Representative western blot using anti-myc antibodies to detect
624 myc-tagged PA-X and tubulin as a loading control. (C) Plot of the relative levels of PA-X after
625 cycloheximide treatment. For each replicate, PA-X protein levels were normalized to tubulin
626 protein levels and reported as the $\log_2$ transformed ratio from time zero. A linear regression was

627 performed for each dataset and the *p* value calculated relative to PR8 PA-X61 (full length PA-
628 X). The lines represent the linear regression and the shaded region indicates the 95% confidence
629 interval (PA-X61: slope = -0.58; confidence interval: -0.87 – -0.28; PA-X41: slope = -0.61,
630 confidence interval = -0.84 – -0.38). $n \geq 3$. The half-life (t1/2) values were calculated as the
631 negative inverse of the slope and are reported in minutes. (D) Levels of PA-X41 mRNA were
632 measured by RT-qPCR. After normalization to 18S rRNA, levels are plotted as amounts relative
633 to time 0. $n > 3$.
634
635 **FIGURE 5: Translation inhibition reduces PA-X-mediated host shutoff, suggesting PA-X is**
636 **likely unstable during infection**
637 (A) Levels of the indicated endogenous RNAs were measured by RT-qPCR in A549 "iPA-X"
638 cells, which express wild-type (wt) PR8 PA-X or a PR8 PA-X catalytic mutant (D108A) under a
639 doxycycline inducible promoter. RNA samples were collected after 14 hours of PA-X induction
640 with doxycyline followed by a 2-hour treatment with 200 μg/mL of cycloheximide (CHX) or
641 vehicle control. After normalization to 18S rRNA, mRNA levels are plotted relative to
642 uninduced wt iPA-X cells (G6PD, TAF7) or relative to induced wt iPA-X cells (PA-X) on a
643 logarithmic scale. $n \geq 3$. *** = $p < 0.001$, ns = $p > 0.05$ 3-way ANOVA followed Tukey's
644 multiple comparisons test. (B) Levels of the indicated endogenous human mRNAs (G6PD and
645 TAF7) and viral RNAs (HA) were measured by RT-qPCR in cells infected with wt PR8 or PR8
646 ΔX at a MOI of 5 for 24 hours prior to a 2-hour treatment with 200 μg/mL of cycloheximide
647 (CHX) to inhibit translation or a vehicle control. After normalization to 18S rRNA, RNA levels
648 are plotted relative to mock infected cells (G6PD, TAF7) or as amounts normalized to cellular
649 18S rRNA (HA) on a logarithmic scale. The dashed lines indicate RNA levels in mock infected

650 cells. n = 3. * = $p < 0.05$, ns = $p > 0.05$, 2-way ANOVA followed by Sidak's multiple

651 comparisons test.

652 **Table 1: Half-lives of PA-X from PR8, pH1N1, Udorn, HK06, and Perth**

PA-X	Slope of linear regression	Half-Life in Minutes	95% confidence interval on slope
A/Puerto Rico/8/1934	-0.70	86	-0.90 to -0.50
A/California/7/2009pdm pH1N1	-0.11	546	-0.35 to 0.12
A/Udorn/307/1973 H3N2	-1.77	34	-2.41 to -1.14
A/Perth/16/2009 H3N2	-0.24	250	-0.78 to 0.30
A/Hong Kong/218847/2006 H1N1	-0.73	83	-1.07 to -0.38

653

654 **Table 2: Primers used in this study**

Purpose	Sequence (5' - 3')
18S qPCR Forward	GTAACCCGTTGAACCCCATT
18S qPCR Reverse	CCATCCAATCGGTAGTAGCG
PA-X qPCR Forward- amplifies BGH 3' UTR region on the vector (Fig 1-4)	GAGTCTAGAGGGCCCGTTTA
PA-X qPCR Reverse- amplifies BGH 3' UTR region on the vector (Fig 1-4)	GAGGGGCAAACAACAGATGG
PA-X qPCR Forward - Fig 5	GCGACAATGCTTCAATCCGA
PA-X qPCR Reverse - Fig 5	TTGACTCGCCTTGCTCATTG
HA qPCR Forward	CTGGACCTTGCTAAAACCCG
HA qPCR Reverse	TCTGGAAAGGGAGACTGCTG
G6PD qPCR Forward	TGAGCCAGATAGGCTGGAA
G6PD qPCR Reverse	TAACGCAGGCGATGTTGTC
TAF7 qPCR Forward	TAGCACTGATCCTAAAGCAAGC
TAF7 qPCR Reverse	GGCAGAGTAATTCCGTGGTTC
Clone PA-X Variants -amplifies CDS starting	CTTAAGCTTGGTACCGGAGTACTGG

from 5’ end vector sequences to clone into pCR3.1 SalI site	
Clone PA-X Variants -amplifies CDS at BGH 3’ UTR to clone into pCR3.1 XhoI site	GTTTAAACGGGCCCTCTAGACTCGA
Make D108A A/HongKong/218847/2006 - mutates active site (Fwd)	CAGAGCTGGCAGAAACTTTGGTTTCTC AGCT
Make D108A A/HongKong/218847/2006 - mutates active site (Rev)	GCCAGCTCTGTATGATTACAAAGAGAA TAGA
Make D108A A/California/7/2009pdm- mutates active site (Fwd)	GTCATACAAAGCAGGAAGAAATTTAG GCTTC
Make D108A A/California/7/2009pdm- mutates active site (Rev)	TTTCTTCCTGCTTTGTATGACTACAAAG AG
Make D108A A/Udorn/307/1972-mutates active site (Fwd)	ATCATACAAAGCTGGCAGAAACTTCGG
Make D108A A/Udorn/307/1972-mutates active site (Rev)	GTTTCTGCCAGCTTTGTATGATTACAA GG
Clone A/Perth/16/2009 PA-X (wt and D108A) - amplifies from 5’ UTR to clone into pCR3.1 SalI site	TAAACTTAAGCTTGGTACCGGAGTACT GGTCGACCCTCCG
Make D108A A/Perth/16/2009 - mutates active site (Rev)	AATCATACAAAGCTGGTAGAAACTTCG G
Make D108A A/Perth/16/2009 - mutates active site (Fwd)	TTTCTACCAGCTTTGTATGATTACAAGG AG
Clone A/Perth/16/2009 PA-X (wt and D108A) - inserts deletion for frameshifting (Rev)	GGACTGACGAAGGAATCCCATAGG
Clone A/Perth/16/2009 PA-X (wt and D108A) - inserts deletion for frameshifting (Fwd)	CCTATGGGATTCCTTCGTCAGTCC
Clone Make D108A A/Perth/16/2009 PA-X (wt and D108A) - amplifies at end of CDS to clone into pCR3.1 MluI site	CTGAGATCAGCTTCTGCTCCACGCGTGA CTTCTTTGGACATTTGAGAAAGCTTGC
Make PR8 PA-X15 - amplifies at 3’ end of truncated CDS to clone into pCR3.1 MluI site	ATCAGCTTCTGCTCCACGCGTGATTTC AAACCTTTCTTCAATTG
Make PR8 PA-X41 - amplifies at 3’ end of truncated CDS to clone into pCR3.1 MluI site	ATCAGCTTCTGCTCCACGCGTGACATA GGCTCTAAAATTTTCAA

Figure 1

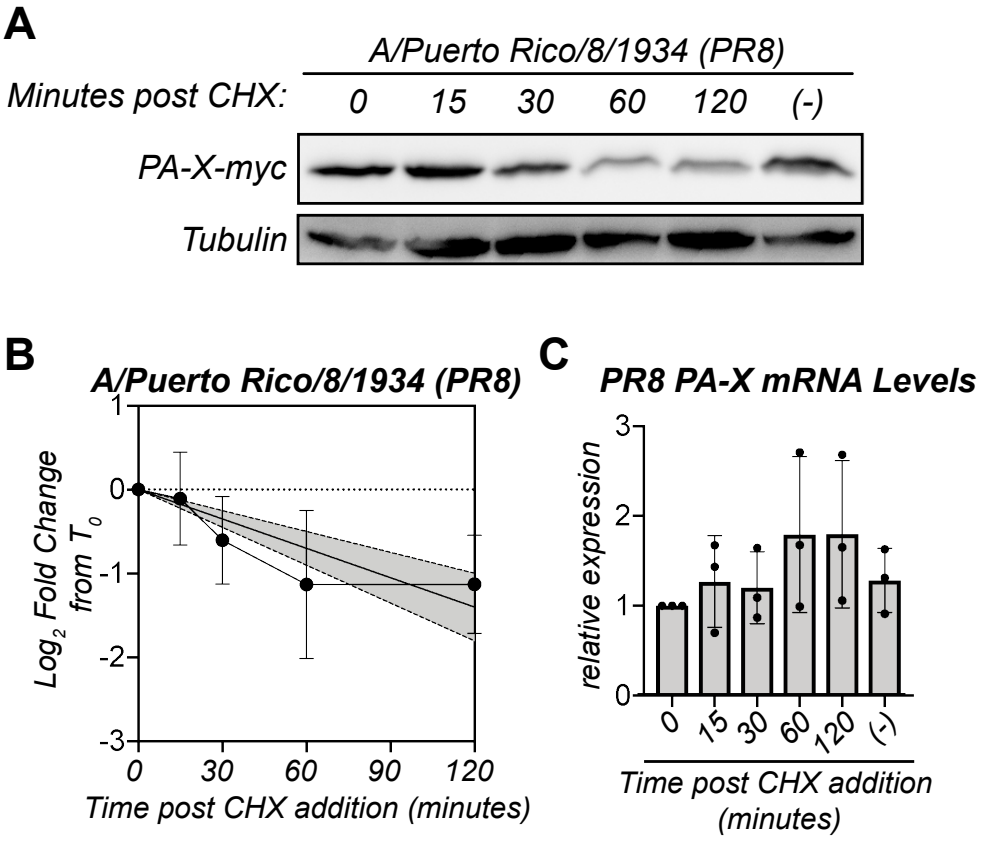

FIGURE 1: PA-X is unstable. (A-C) Protein and RNA samples were collected from HEK293T cells expressing the catalytically inactive PR8 PA-X at the indicated time points after treatment with 200 µg/mL of cycloheximide (CHX) to inhibit translation. (-) indicates vehicle-treated cells collected at 120 minutes. (A) Representative western blot using anti-myc antibodies to detect myc-tagged PA-X and tubulin as a loading control. (B) Plot of the relative levels of PA-X after cycloheximide treatment. For each replicate, PA-X protein levels were normalized to tubulin protein levels and reported as the log2 transformed ratio relative to time 0. The line represents the linear regression and the shaded region its 95% confidence interval. n = 7 (C) Levels of PA-X mRNA were measured by RT-qPCR. After normalization to 18S rRNA, levels were plotted as amounts relative to time 0. n = 3.

Figure 2

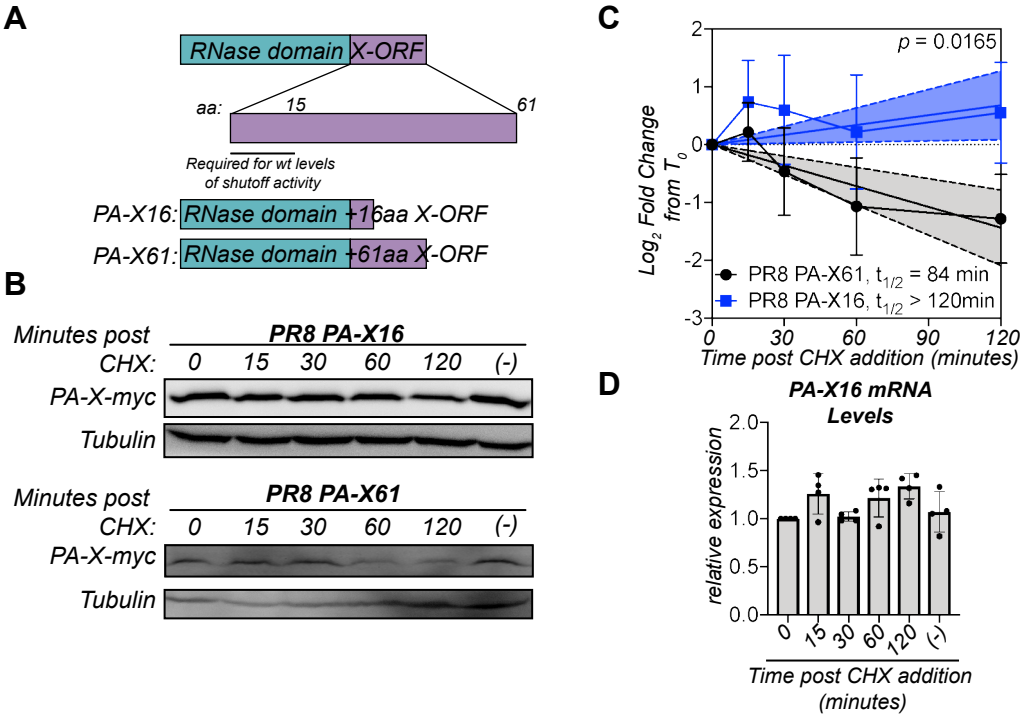

FIGURE 2: The X-ORF mediates PA-X instability

(A) Schematic diagram of PA-X domains and PR8 PA-X16 truncation used. (B-D) Protein and RNA samples were collected from HEK293T cells expressing the catalytically inactive full-length or truncated C-terminally myc-tagged PA-X at the indicated time points after treatment with 200 µg/mL of cycloheximide (CHX) to inhibit translation. (-) indicates vehicle-treated cells collected at 120 minutes. (B) Representative western blot using anti-myc antibodies to detect myc-tagged PA-X and tubulin as a loading control. (C) Plot of the relative levels of PA-X after cycloheximide treatment. For each replicate, PA-X protein levels were normalized to tubulin protein levels and reported as the log2 transformed ratio from time 0. A linear regression was performed for each dataset and the p value calculated relative to PR8 PA-X61(full length PA-X). The lines represent the linear regression and the shaded regions indicate the 95% confidence interval (PA-X61: slope = -0.72, confidence interval = -1.04 – -0.39; PA-X16: slope = 0.34, confidence interval = 0.04 –0.64). The half-life (t1/2) for PA-X61 was calculated as the negative inverse of the slope and is reported in minutes. As the slope for PA-X16 is positive, the half-life of this protein cannot be calculated and is therefore reported simply as longer than the time course of the experiment. n ≥ 3 (D) Levels of PA-X16 mRNA were measured by RT-qPCR. After normalization to 18S rRNA, levels are plotted as amounts relative to time 0. n > 3.

Figure 3

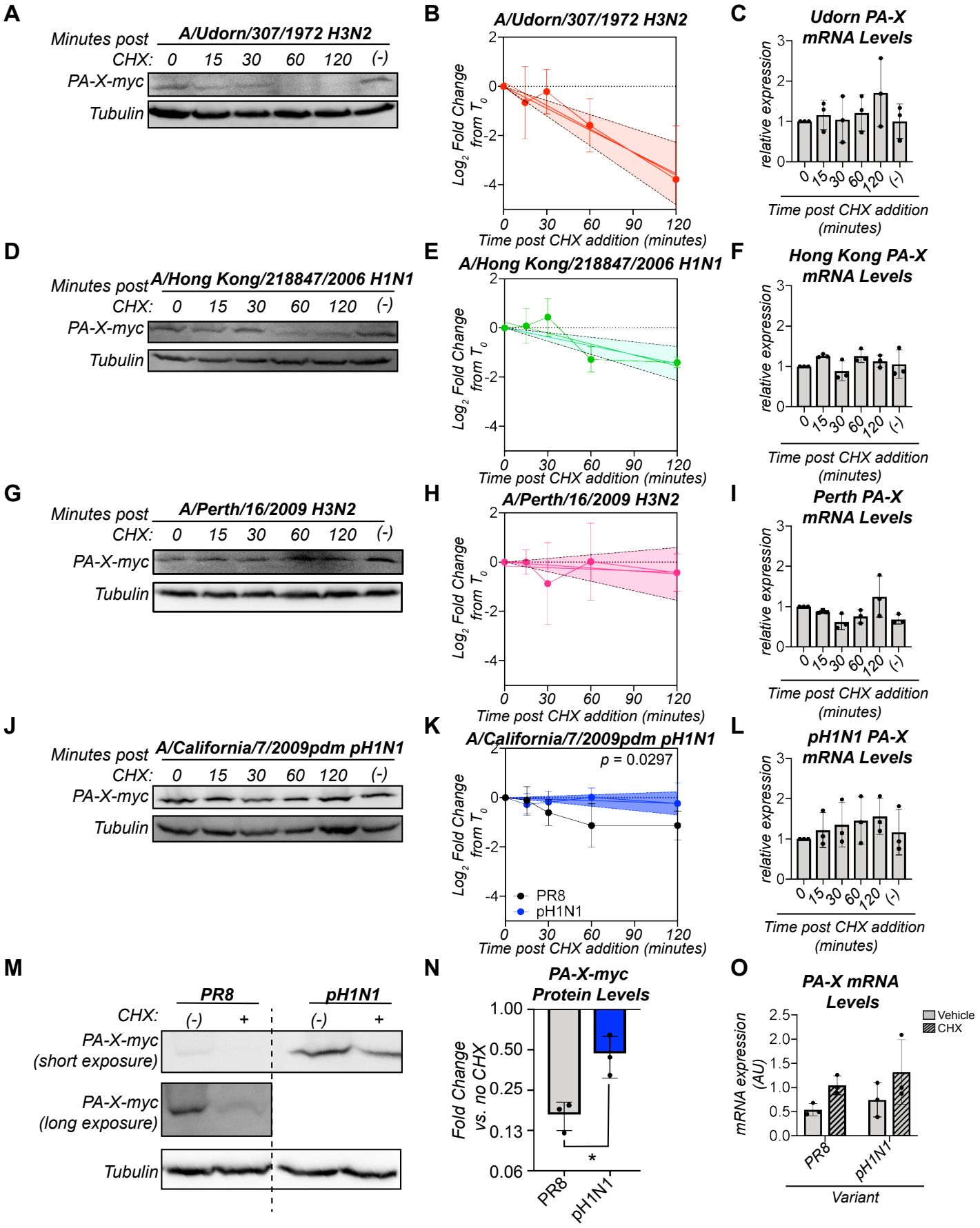
A
Minutes post CHX:
A/Udorn/307/1972 H3N2
0 15 30 60 120 (-)
PA-X-myc
Tubulin
B
A/Udorn/307/1972 H3N2
Log2 Fold Change from T0
Time post CHX addition (minutes)
C
Udorn PA-X mRNA Levels
relative expression
Time post CHX addition (minutes)
D
A/Hong Kong/218847/2006 H1N1
E
A/Hong Kong/218847/2006 H1N1
F
Hong Kong PA-X mRNA Levels
G
A/Perth/16/2009 H3N2
H
A/Perth/16/2009 H3N2
I
Perth PA-X mRNA Levels
J
A/California/7/2009pdm pH1N1
K
A/California/7/2009pdm pH1N1
p = 0.0297
PR8
pH1N1
L
pH1N1 PA-X mRNA Levels
M
PR8
pH1N1
(-) +
PA-X-myc (short exposure)
PA-X-myc (long exposure)
N
PA-X-myc Protein Levels
Fold Change vs. no CHX
*
O
PA-X mRNA Levels
Vehicle
CHX
mRNA expression (AU)
Variant

FIGURE 3: The stability of PA-X varies among influenza A virus strains.
Protein and RNA samples were collected from HEK293T cells expressing the catalytically inactive C-terminally myc tagged PA-X from indicated strain at the indicated time points (A-L) or 4 hours (M-O) after treatment with 200 µg/mL of cycloheximide (CHX) to inhibit translation. (-) indicates vehicle-treated cells collected at 120 minutes (A-L) or 4 hours (M-O). (A, D, G, J, M) Representative western blot using anti-myc antibodies to detect myc-tagged PA-X and tubulin as a loading control. (B, E, H, K) Plot of the relative levels of PA-X after cycloheximide treatment. For each replicate, PA-X protein levels were normalized to tubulin protein levels and reported as the log2 transformed ratio from time zero. The line represents the linear regression and the shaded region its 95% confidence interval. n = 3 for each variant. In K, the PR8 PA-X dataset from Figure 1 is included for comparison and the reported p value is relative to PR8 PA-X. Two of the three pH1N1 PA-X replicates were performed in parallel with PR8 PA-X. (N) Plot of average change in PA-X levels after 4-hour cycloheximide treatment. For each replicate, protein levels of PA-X were normalized to tubulin protein levels and reported as the fold change vs. vehicle-treated PA-X expressing cells. * = $p < 0.05$, Student's t-test. n = 3. (C, F, I, L, O) Levels of PA-X mRNA were measured by RT-qPCR. After normalization to 18S rRNA, levels are plotted as amounts relative to time 0 (C, F, I, L) or as arbitrary units (O). n = 3.

Figure 4

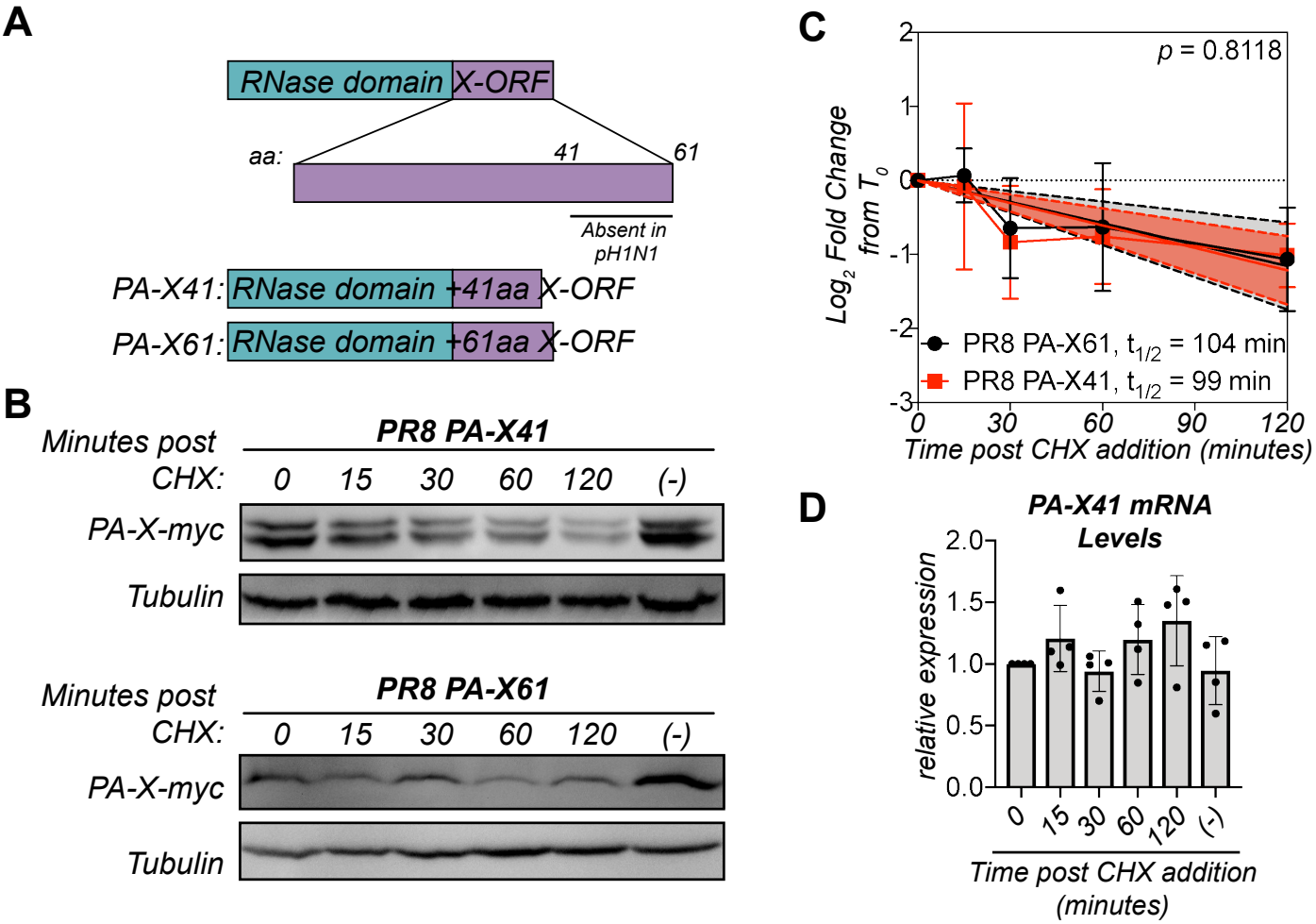

FIGURE 4: The length difference between the two major variants of the PA-X X-ORF does not account for differences in PA-X instability.
(A) Schematic diagram of PA-X domains and PR8 PA-X41 truncation used. (B-D) Protein and RNA samples were collected from HEK293T cells expressing the catalytically inactive truncated or full-length C-terminally myc-tagged PA-X at the indicated time points after treatment with 200 µg/mL of cycloheximide (CHX) to inhibit translation. (-) indicates vehicle-treated cells collected at 120 minutes. (B) Representative western blot using anti-myc antibodies to detect myc-tagged PA-X and tubulin as a loading control. (C) Plot of the relative levels of PA-X after cycloheximide treatment. For each replicate, PA-X protein levels were normalized to tubulin protein levels and reported as the log2 transformed ratio from time zero. A linear regression was performed for each dataset and the p value calculated relative to PR8 PA-X61 (full length PA-X). The lines represent the linear regression and the shaded region indicates the 95% confidence interval (PA-X61: slope = -0.58; confidence interval: -0.87 – -0.28; PA-X41: slope = -0.61, confidence interval = -0.84 – -0.38). $n \geq 3$. The half-life (t1/2) values were calculated as the negative inverse of the slope and are reported in minutes. (D) Levels of PA-X41 mRNA were measured by RT-qPCR. After normalization to 18S rRNA, levels are plotted as amounts relative to time 0. $n > 3$.

Figure 5

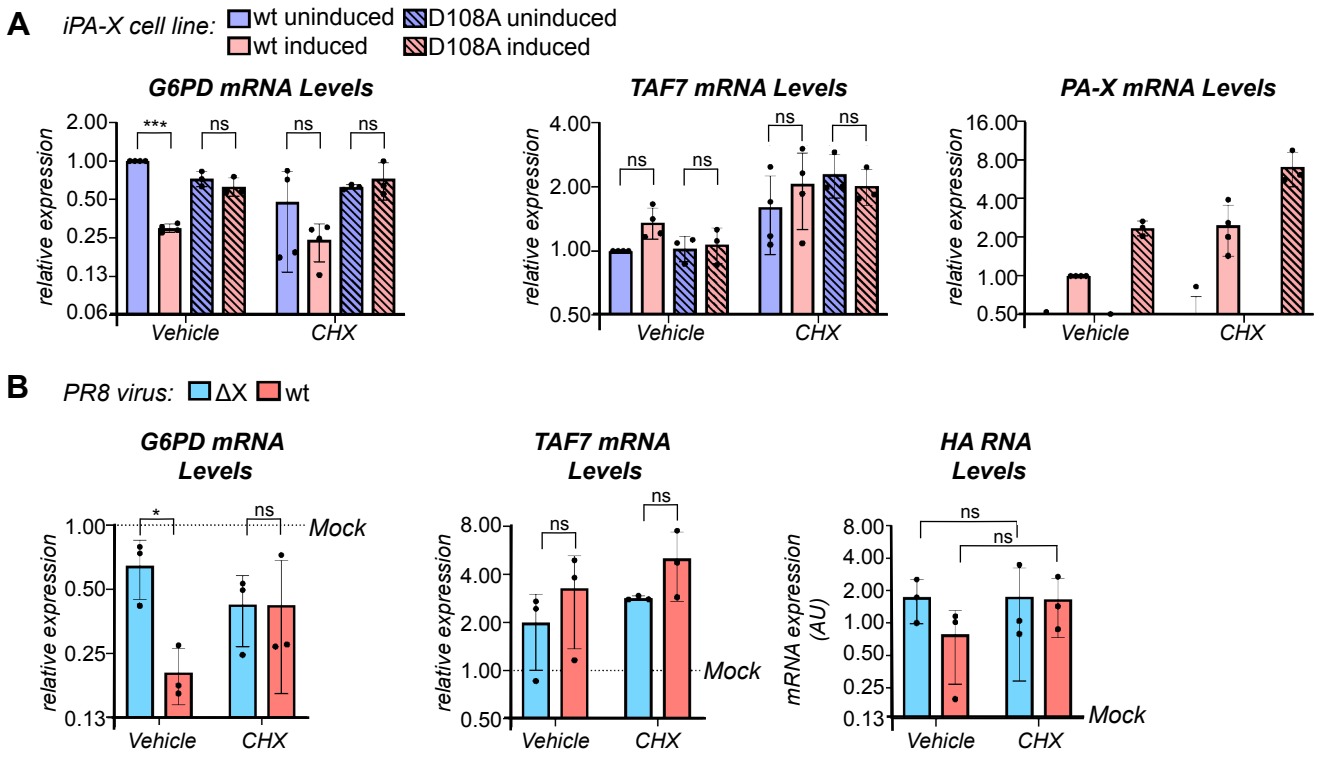

FIGURE 5: Translation inhibition reduces PA-X-mediated host shutoff, suggesting PA-X is likely unstable during infection. (A) Levels of the indicated endogenous RNAs were measured by RT-qPCR in A549 "iPA-X" cells, which express wild-type (wt) PR8 PA-X or a PR8 PA-X catalytic mutant (D108A) under a doxycycline inducible promoter. RNA samples were collected after 14 hours of PA-X induction with doxycyline followed by a 2-hour treatment with 200 µg/mL of cycloheximide (CHX) or vehicle control. After normalization to 18S rRNA, mRNA levels are plotted relative to uninduced wt iPA-X cells (G6PD, TAF7) or relative to induced wt iPA-X cells (PA-X) on a logarithmic scale. n ≥ 3. *** = $p < 0.001$, ns = $p > 0.05$ 3-way ANOVA followed Tukey's multiple comparisons test. (B) Levels of the indicated endogenous human mRNAs (G6PD and TAF7) and viral RNAs (HA) were measured by RT-qPCR in cells infected with the wt PR8 or PR8 ΔX at a MOI of 5 for 24 hours prior to a 2-hour treatment with 200 µg/mL of cycloheximide (CHX) to inhibit translation or a vehicle control. After normalization to 18S rRNA, RNA levels are plotted relative to mock infected cells (G6PD, TAF7) or as amounts normalized to cellular 18S rRNA (HA) on a logarithmic scale. The dashed lines indicate RNA levels in mock infected cells. n = 3. * = $p < 0.05$, ns = $p > 0.05$, 2-way ANOVA followed by Sidak's multiple comparisons test.